SPIN
Vol. 11, No. 4 (2021) 2150028 (16 pages)

DOI: 10.1142/S2010324721500284

World Scientific
www.worldscientific.com

Modeling and Simulation of Magnons Scattering Across Shear Spins in Multilayered Ferromagnetic Slabs

Leila Ferrah
Research Unit: Materials, Processes and Environment
M'hamed Bougara University, Boumerdes, Algeria
l.ferrah@univ-boumerdes.dz

Boualem Bourahla
Laboratory of Physics and Quantum Chemistry
M. Mammeri University, BP 17 RP, Tizi-Ouzou, Algeria
bourahla_boualem@yahoo.fr; boualem.bourahla@ummto.dz

Salah Blizak
Research Unit: Materials, Processes and Environment
M'hamed Bougara University, Boumerdes, Algeria
s.blizak@univ-boumerdes.dz

Received 2 June 2021
Accepted 20 November 2021
Published 18 January 2022

In this work, we introduce a computer model and theoretical approach based on the matching technique to investigate the spin precession and the magnetic properties of an ordered magnetic interface joining two ferromagnetic multilayers of type AB, made of 10 spin slabs, obtained by alternative two spin layers A and B. We simulate, particularly, the coherent magnon transmission through spins' interface, in multilayered thin films, obtained by shearing a part of the film from the other at an angle of 30°. The individual and total transmittance of bulk magnons of the thin film, scattering coherently at the shearing interface zone and the localized magnonic spin states, are calculated and analyzed. The transmission and reflection spin modes are derived as elements of a Landauer–Büttiker type scattering matrix. The results highlight the localized spin states on the interface shear domain and their interactions with incident magnons. The evolutions of the magnonic spectra can be presented for arbitrary directions of the incident magnons on the boundary zone, for all accessible frequencies in the propagating bands as well as for the magnetic exchange coupling between each spin A(B) and its adjacent sites and their spin intensity. The results demonstrate the dependence of the magnonic spectra for the perfect multilayered films and at the inhomogeneous domain of the interface shear. The analysis of the spectra illustrates the fluctuations, related to Fano resonances, due to the coupling between travelling magnons and the localized modes in the shear interface domain. The calculated spectra could yield useful information concerning the magnetic parameters of such interface slabs in multilayered films.

Keywords: Ferromagnetic interface; magnons' transmission and reflection; localized spin states.

1. Introduction

In the last decades, technological progress and the development of deposition techniques have led to the creation of miniaturized artificial magnetic layers and multilayers.[1,2] It is stated that the thickness of the films, which is composed of artificial lattices, is at the origin of their extraordinary magnetic properties.[3] The objective of the miniaturized systems is to increase the storage capacity of memories, while consuming much less energy.[4] Moreover, before making applications in different domains,[5] it is necessary to understand the fundamental characteristics of the artificial films and to advise means to control their magnetic behavior. This could be achieved by studying the spin waves' propagation and scattering phenomena.

The spin excitations, magnon dispersions and spinwaves' behavior are very different from those of the conventional massif structures. Consequently, magnons' spectra and magnetic properties depend on the details of their structure at the atomic scales.[6]

The study of spin dynamics and precessional motion in perturbed small-scale lattice requires, imperatively, knowledge of spin excitations in its perfect film, to satisfy the periodic boundary condition.

The singularity of spin excitations in film minces and superlattices are at the basis of their uses in modern applications.[7] Restricting the dimensions or disturbing the geometry of such systems can accentuate the peculiarities of the spins' behavior and the motion of precession, resulting in very interesting magnetic properties.[8,9] It is reported that the spin scattering process and localization magnons' phenomena in mesoscopic lattices have interested several authors from a long time.[10] Two fundamental elements in undertaking any theoretical investigation of spin motion are required to process: Spin precession description and spinwave dispersions in ferromagnetic nanostructured layers or multilayers. The first one is the knowledge of the magnetic exchange, between spin sites in the unit cell. The second is essential to build the spin dynamics matrix, by developing an appropriate scheme allowing us to describe the scattering phenomena by inhomogenous spin sites and defect zones. To deal with the problem of spin dynamics in thin magnetic films, in the presence of inhomogeneous spin sites or disturbed zones, we use one of the three theoretical approaches that are available in the literature, allowing to point out the defect impacts and the breaking symmetry effects. Especially, the Slab method, the green functions and the matching method. The last technique has been applied successfully, by our research team, to study several structures with breaks in symmetry,[11–13] furthermore isolated nanostructures,[14,15] in phononic, magnonic and electronic domains.

In this work, we report the impact of the spin interface sites on the collective excitation of the spins in ferromagnetic multilayers made from 10 parallel spin layers. The purpose is to understand the mechanisms that govern the precession motion of spins at the interface zone in the composite AB thin film, in the presence of perturbed region by using the matching approach.[16–18] For the simulated model, we symbolize the film by the succession of two different spin planes A and B, distanced by an interatomic distance a. We determine, particularly, the magnonic spectra (transmission/reflection, localized spin states and spin transmittance) generated by the interface domain, obtained by shearing a part of the film from the other at an angle of 30°, along x-direction.

The magnonic spectra, along a particular direction (30°), have not been studied until now. On the other hand, if the shear angle is 45°, we obtained a stepped structure which is discussed by some authors.[12,16,19,20]

The structural form of this paper is as follows. In Sec. 2, we describe the multilayer film considered to compute the suggested model calculations.

In Sec. 3, we give the matching technique principle, applied in our study to deal with the localization phenomena and spinwaves' scattering.

In Sec. 3.1, we start with a reminder of the theory that governs the spin excitations in ferromagnetic multilayered perfect film, which permit access to dispersion relations and the group velocities of the multilayered slabs of the type AB.

In Sec. 3.2, we are interested in the interface spins' dynamics and scattering in the shearing interface domain itself. We determine, principally, the localized magnon branches, the transmission and reflection coefficients as well as the magnonic transmittance.

In Sec. 4, numerical applications are presented and discussed for the studied shearing interface zone, in ferromagnetic multilayered film, made by 10 atomic spin layers, constructed from alternate two types of layers A and B. The spinwaves propagating

through shear spins in multilayered ferromagnetic slab is examined by using all parameters describing the interface domain. The conclusion of this work is presented in the last section.

2. Ferromagnetic Multilayer Film Description

The model ferromagnetic thin film, studied in this article, is made up of 10 spin layers, obtained by alternating two types of layers A and B. The multilayer film exhibits a spin interface resulting from shearing one part of the film relative to the other at an angle of 30°. Our main interest is to study the behavior of spin waves in lamellar magnetic multilayers A and B. The motivation comes from the fact that this type of film constitutes the geometric basis of magnonic crystals. They can be expected to be used as elements of sensors and magnetic valves. The behavior of spin waves in monatomic multilayer has been widely studied in recent years. The presence or the arrangement of two types of atoms (or more) in a lattice or thin film generates interesting phenomena; we can mention the following:

— More multiple reflections are to be expected by the second type of atom B, thus leading to the observation of several resonators, and this is less evident in a monatomic lattice.
  In this figure, the dimensions of the film in the x and y directions are considered sufficiently large (infinite), while its thickness is finite along the z-axis; therefore, it presents a broken symmetry.
  In the perfect region of the multilayered ferromagnetic film, each atomic site p is occupied by the spin vector $\vec{S}_p$, interacting with its nearest neighbors, by the magnetic exchange constants J_{AA} and J_{BB}, respectively, in
— In the A and B layers, the number and the nature of the branches of the localized spin states are very important.
— By mastering the difference between the intensity vectors of spins A and B, we are able to control the width of the magnon forbidden band in the structure.

The two slabs located on either side of the interface are envisaged as perfect waveguides for incident and scattered magnons; whereas, the interface zone is treated as a scattering region. A typical 2D cross section of the studied model is shown in Fig. 1. The same type of spin layers A and B.

In addition, the interactions between the nearest and next nearest spin neighbors of the two types of spin layers A and B are labeled $J_{1\mathrm{AB}}$ and $J_{2\mathrm{AB}}$, respectively.

For the spin sites located in the shearing region of the film, the magnetic interactions can be different from those of the perfect zones. They are characterized by the exchange constants J_{AAd}, J_{BBd}, J_{1ABd} and J_{2ABd}, as indicated in the schematic representation given in Fig. 1.

To simplify the notation of the normalized frequencies of the studied model film, we introduce the following ratios:

$$\begin{cases} r_B = \dfrac{J_{BB}}{J_{AA}}, \quad r_1 = \dfrac{J_{1AB}}{J_{AA}}, \\ r_2 = \dfrac{J_{2AB}}{J_{AA}}, \quad r_{Ad} = \dfrac{J_{AAd}}{J_{AA}}, \\ r_{Bd} = \dfrac{J_{BBd}}{J_{AA}}, \quad r_{1d} = \dfrac{J_{1ABd}}{J_{AA}}, \\ r_{2d} = \dfrac{J_{2ABd}}{J_{AA}}, \quad S = \dfrac{S_B}{S_A}. \end{cases} \tag{1}$$

To perform the simulations and numerical calculations for the ferromagnetic multilayer film, we examine three possibilities of the ratio S of spin intensities in multilayer film ($S_A < S_B$, $S_A = S_B$, $S_A > S_B$).

In addition, for each S value, we consider three probabilities of magnetic coupling between spin sites in the film. These possibilities are as follows:

(i) Softening coupling (corresponds to the case where the magnetic exchanges in the interface domain are smaller than those of perfect slabs located on both sides of the scattering zone).
(ii) Homogenous interactions (the spin interactions are taken identical everywhere).
(iii) Hardening situation (the exchange integrals in the interface domain are greater than those of perfect slabs).

For the numerical simulations, we have chosen variations of the order of 10% between the physical parameters which characterize the perturbed film compared to the perfect one.

Explicitly, the numerical analysis is carried out for three possibilities of the spin intensity (S greater or smaller about 10%) and the magnetic coupling that determine a choice of the spin environment of the sheared atomic sites (10% higher or 10% lower), which is a reasonable situation.

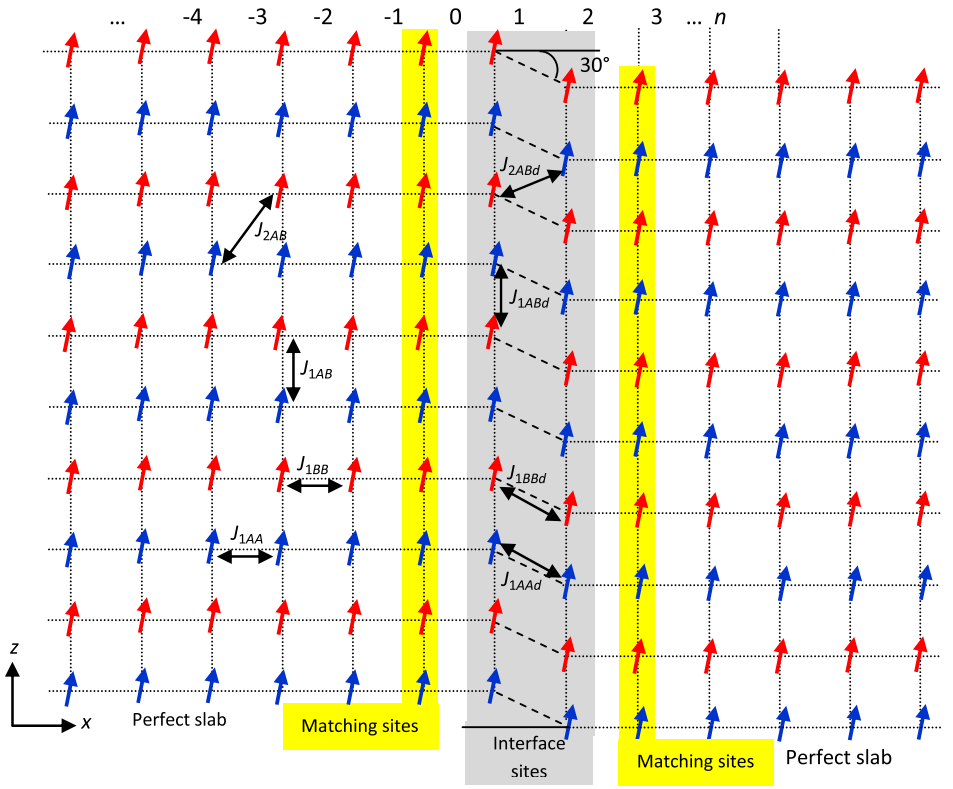

Fig. 1. A schematic representation showing a 2D cross section of the multilayered thin film with a spin interface, according to the matching method concept. The interface domain is the cry area; whereas, the matching regions are colored yellow. The interface, identified as an inhomogenous zone, is obtained by shearing a part of the multilayered film from the other at an angle of 30° (Color online).

Although the possibilities (spin intensity and the interaction environment values (softening, homogeneous and hardening)) do not correspond to exact values, which may be significant in some magnetic metals, each choice is a reasonable working value to illustrate our calculations.

3. Matching Technique Principle

Historically, the matching method was introduced in the sixties by Feuchtwang.[21] Later, it was revisited by Szeftel *et al.* in two different articles,[22,23] which deal with the surface phonon problems:

(i) The first paper is entitled "Calculation of surface phonons and resonances: the matching procedure revisited: I", published in 1987.
(ii) The second, published in 1988, under the title "Calculation of surface phonon dispersion on Ni(100) and Ni(100) + c(2 × 2) along the (010) direction by means of the matching procedure: II".

In the magnonic domain, Tamine applied the method,[24] in 1996, to determine the localized spin states generated by spin precessions at the surface of antiferromagnetic simple cubic structure with frustrations.

Eight years later,[25] the matching technique was extended to deal with spinwaves' scattering phenomena.

In both domains (phononic and magnonic), the matching method returns account in a satisfactory way for the phonons and magnons' dispersion curves, the localized states generated by the surface and the scattering phenomena. Moreover, the method gives a more precise definition of the resonance concept and permits an easy analysis of the behavior of the elementary excitations near the disturbed zones.

However, its implementation necessarily involves the subdivision of the crystal into three different zones (perfect, inhomogenous and matching).

In this work, with a view to simplify understanding, we present a 2D cross section of the studied multilayered thin film, in Fig. 1. The illustration defines the three regions according to the matching procedure. For more information and details, refer to Refs. 21–23.

3.1. *Spin excitations in ferromagnetic multilayered perfect film*

3.1.1. *Spin precession and magnons' dispersion relations*

For Heisenberg ferromagnetic exchange interactions between adjacent spins $\vec{S}_p$ and $\vec{S}_{p'}$, located at the spin sites p and p', respectively, the Hamiltonian is given by the following expression:

$$H = -\sum_{p \neq p'} J_{pp'} \vec{S}_p \vec{S}_{p'}. \quad (2)$$

The quantities $\vec{S}_p(\vec{S}_{p'})$ are vectors, and the constant $J_{pp'}$ is the exchange integral coupling between magnetically nearest neighbor spins p (p'). It is strongly depending on the position of the spin site in the considered film. The exchange integrals are uniform, in two perfect slabs located on either side of the interface space, except in the interface domain itself, where the exchange integrals can take a different value from the rest of the perfect slabs.

To determine the spin dynamics of the multilayer films, either the perfect one or the one containing the scattering region, we apply Eq. (2).

If we consider that the spin positions p and p' are inside the semi-infinite perfect slabs, far from the interface region, all the equations of the spin precessions' motion can be grouped together in the following matrix form:

$$[\Omega I - D(S, r_B, r_1, r_2, \eta, \exp(i \times \phi_y)]|u\rangle = |0\rangle. \quad (3)$$

In Eq. (3), $|u\rangle$ is a vector that regroups all spin precession amplitudes in a unit cell, I designs an identity matrix and D denotes the spin dynamics matrix of the ferromagnetic perfect multilayer.

The quantities $\eta \equiv e^{i\phi x}$ and $e^{i\phi y}$ constitute Bloch phase factors that liaise neighboring sites, respectively, in x and y directions. Over the first Brillouin zone, the normalized dimensionless wavevectors are given by $\phi_x = q_x a$ and $\phi_y = q_y a$, where a is the lattice parameter. The doublet (q_x, q_y) constitutes the reciprocal lattice wavevector associated with (ϕ_x, ϕ_y). The ration $\Omega = \frac{\omega}{\omega_0}$ defines the dimensionless frequency of the ferromagnetic film, where ω represents the pulsation of spin film precession and ω_0 is its characteristic pulsation.

Note that ω_0 is not identical for A and B spin layers, $\omega_{0A} = [\frac{\hbar}{J_{AA} S_A}]^{-1}$ and $\omega_{0B} = [\frac{\hbar}{J_{BB} S_B}]^{-1}$.

By resolving Eq. (3), we get access to the eigenfrequencies Ω_ν as well as the corresponding eigenvectors $\vec{u}_\nu$ of the perfect multilayer films.

In order to illustrate the spin dynamics in the considered multilayer model film, we have presented, in Fig. 2, the spin dispersion curves $\Omega(\phi_x)$. These curves are plotted as a function of the normalized wavevector ϕ_x and at a given value of ϕ_y.

In the perfect films, the spin magnon modes are propagating and verify the generic phase factor condition $|\eta| = 1$, between adjacent spin sites.

Furthermore, to analyze the localized magnonic branches, the scattering process and the spinwaves' transmission via the spin sites located in the shearing zone, we need all solutions of Eq. (3). The latter represents the propagating or the evanescent eigenmodes of the spin dynamics matrix.

Additionally, in all cases, the two types of spin modes may be described by the doublet (η, η^{-1}). To determine them, different procedures are proposed in the literature.[26,27]

Having a nontrivial solution for the matrix of Eq. (3), it is imperative to take its determinant equal to zero,

$$\det[\Omega I - D(S, r_B, r_1, r_2, \eta, \exp(i \times \phi_y)] = 0. \quad (4)$$

Therefore, we obtain a secular equation of degrees 10 in η that is expressed in the polynomial form

$$\sum_{s=1}^{10} C_s \eta^s = 0. \quad (5)$$

The coefficients C_s are expressed in Ω, ϕ_y and ϕ_z.

Owing to the Hermitian nature of the spin dynamics of the perfect film, the phase factors η and their inverses η^{-1} verify the polynomial of Eq. (5).

The evanescent spin modes are determined by the condition $|\eta| \prec 1$. The inverse condition, $|\eta| \succ 1$, defines nonphysical divergent modes. To describe spin dynamics in sheared multilayer ferromagnetic film, we consider, only, physically acceptable solutions obtained from the roots of Eq. (5).

3.1.2. *Magnon group velocity*

At the movement of a packet of waves, in a medium, we associate a speed that allows describing the circulation of information and the transport of energy in this medium. This is called the group speed, denoted as V_g. It depends on the variation of the real

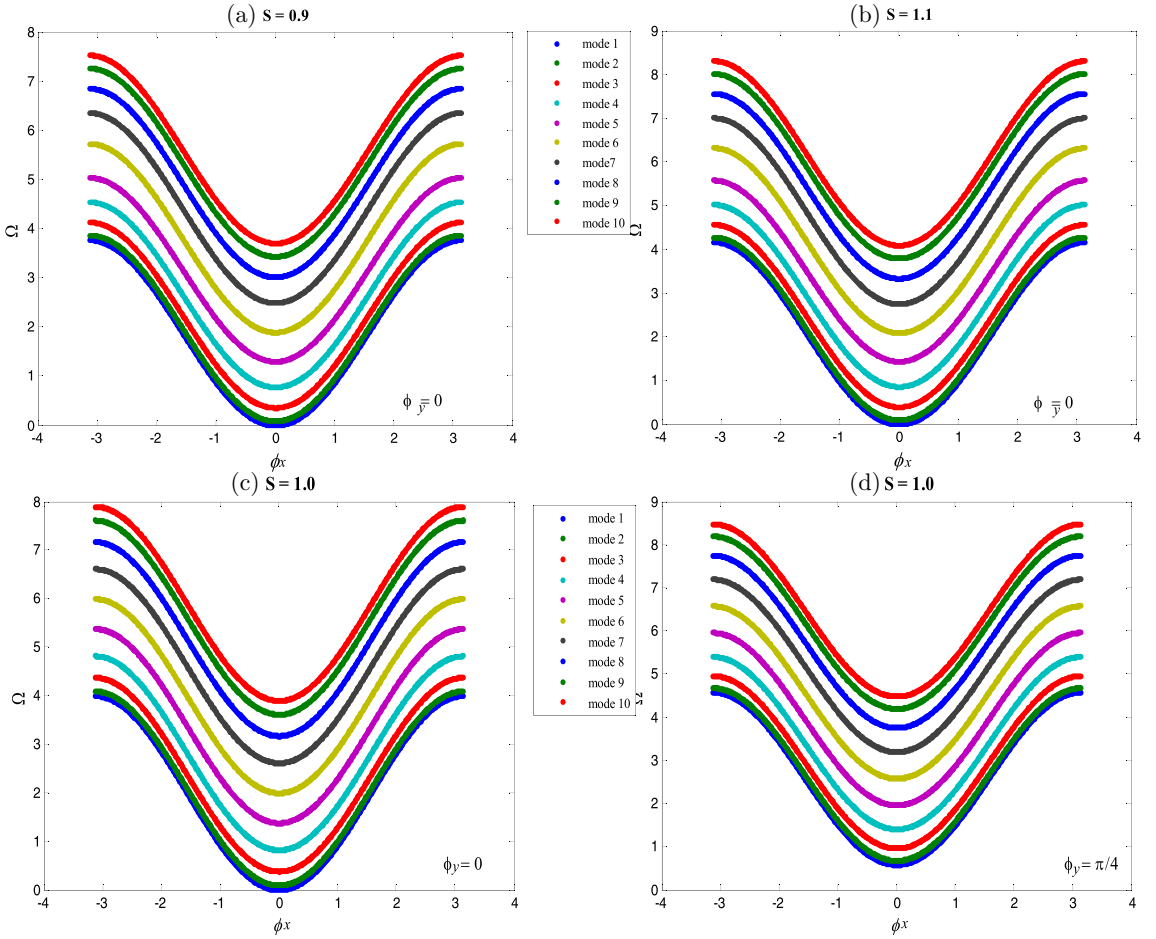

Fig. 2. Magnons' dispersion curves on a multilayer waveguide composed of 10 atomic planes, with ferromagnetic order, presented over the first Brillouin zone, defined by the interval $\phi_x = [-\pi/a, +\pi/a]$. (a) The spin intensity ratio $S = 0.9$ and the normal incidence $\phi_y = 0$, (b) the spin intensity ratio $S = 1.1$ and the normal incidence $\phi_y = 0$, (c) the spin intensity ratio $S = 1.0$ and the normal incidence $\phi_y = 0$, (d) the spin intensity ratio $S = 1.0$ and the oblique incidence $\phi_y = \pi/4$.

wavenumber, in direct relation with the frequency. It is expressed by

$$V_g = \frac{\partial \Omega}{\partial \phi_x}\bigg|_{\phi_y}. \tag{6}$$

If ϕ_x is not a real number, we impose $V_g = 0$.

To determine the group velocities, several calculation techniques can be employed.[28,29]

When the wavevector modulus is of the order of the inverse of the lattice parameter (1/a), and due to the breaking symmetry of the film (interface zone), the dispersion relation $\Omega(\phi_x, \phi_y)$ increases less quicker with ϕ_x.

In the studied interface, given in Fig. 1, we report that the energy flux of magnons per unit area is due to spin waves moving from left to right through a spin layer (yz).

The curves of the group velocities for the perfect multilayer waveguides are plotted in Fig. 3, as a function of the normalized energy Ω.

3.2. *Interface spins' dynamics and scattering*

The spin precessions at the interface domain of the studied film generate infinite number of coupled equations on either side of the scattering zone.

To deal with the problem and describe the dynamics of the disturbed film spins, it is mandatory to decouple the dynamics of a set of irreducible spin sites, which are connected to the boundary sites, from the rest of the system.

The motion of each spin depends on the coordination and the number neighbor sites. Consequently, the shearing angle must be taken into

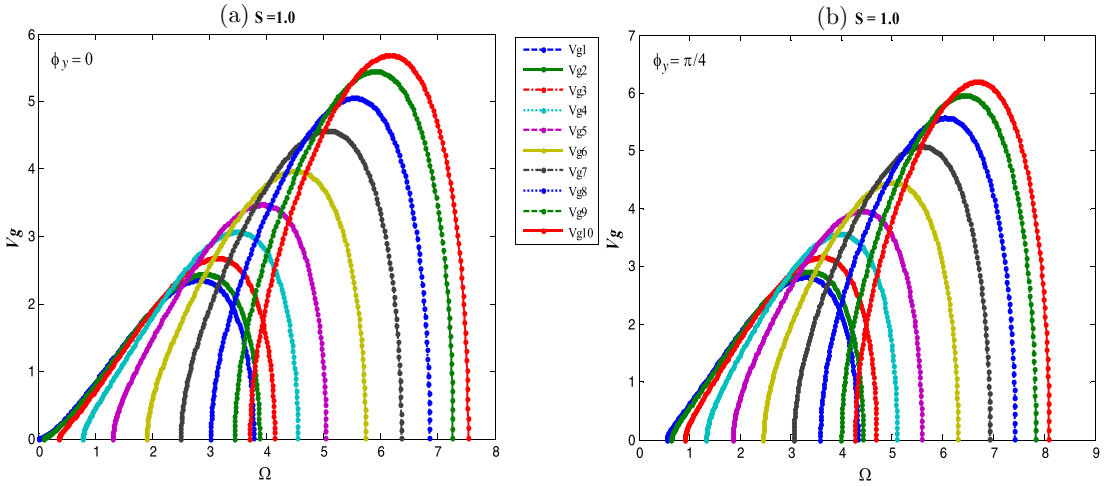

Fig. 3. Curves of the group velocities (V_g) of the perfect multilayer thin film, as function of the scattering frequency Ω. (a) For the normal incidence $\phi_y = 0$, (b) for the oblique incidence $\phi_y = \pi/4$.

consideration when writing the equations of motion of the spin precessions located on either side of the sheared zone (these equations constitute the dynamic matrix of the disturbed system).

3.2.1. *Coherent magnon transmission across the interface*

To specifically examine the spin scattering phenomena via the interface zone, schematized in Fig. 1, we use the propagating and evanescent solutions of Eq. (5). They are given by $|\eta| \leq 1$. The analysis is carried out by the matching procedure.[16–18]

The evanescent spin modes do not transport any energy, but they are essential for mathematically describing the scattering problem and for making a correspondence between the solutions on both sides of the interface zone.

Since the multilayer perfect films do not couple between the spin eigenmodes, we can therefore treat the scattering process for each spin eigenmode individually.

For a given spin mode, denoted by η_i, incident at a frequency Ω and propagating from the left film to the right one, via the interface zone, in the x-direction, the spin scattering due to the interface domain could be considered as coherent reflected and transmitted parts.

For the spin sites belonging to the perfect waveguide located at the left of the nanojunction, the Cartesian components α of the precession field, denoted as $u_{\alpha A}(n, m, l)$, can be expressed as the sum of an incident propagating spinwave and a superposition of the reflected eigenmodes, moving in opposite sense, in the left perfect waveguide, at frequency Ω and fixed direction ϕ_y. We can write them as follows:

$$u_{\alpha A}(n, m, l) = \eta_i^n u_i + \sum_{i'} R_{ii'} \eta_{i'}^{-n} u_{i'}, \quad n \leq -2. \tag{7}$$

For a spin site belonging to the perfect multilayer film, at the right of the interface domain, the rotation spin amplitude $u_{\alpha B}(n, m, l)$ may be expressed as a superposition of the eigenmodes of the perfect waveguide, as follows:

$$u_{\alpha B}(n, m, l) = \sum_{j} T_{ij} \eta_j^n u_j, \quad n \geq 3. \tag{8}$$

The vectors u_j and $u_{i'}$ are the eigenvectors of the spin dynamics matrix of perfect multilayer waveguide films at the dimensionless energy Ω. The notations $R_{ii'}$ and T_{ij} designate, respectively, the reflection and transmission amplitudes describing the scattering process of an incident spinwave i to the eigenmodes i' (for the reflection) and the eigenmodes j (for the transmission).

Note that the knowledge of coefficients $R_{ii'}$ and T_{ij} allows entire determination of the solutions of Eqs. (7) and (8).

By considering a Hilbert space for the scattering zone and denoting by $[|\vec{R}\rangle, |\vec{T}\rangle]$ the basis vectors related to the reflection and transmission coefficients and by $|\vec{u}_{\text{int}}\rangle$ the spin fluctuations of the irreducible sites of the interface region, the equations of motion for the scattering spin sites, coupled to the rest of

the spins of the ferromagnetic film, may be expressed as terms of the vector $[|\vec{u}_{\rm int}\rangle, |\vec{R}\rangle, |\vec{T}\rangle]$.

By introducing appropriate transformations, which relate to the spin rotation amplitudes in Eqs. (7) and (8), we obtain an inhomogeneous square matrix, of the perturbed film, expressed in the following form:

$$[\Omega I - D(S, r_B, r_1, r_2, r_{Bd}, r_{1d}, r_{2d}, \eta, \exp(i \times \phi_y)] \times [|\vec{u}_{\rm int}\rangle, |\vec{R}\rangle, |\vec{T}\rangle] = -|i\vec{n}h\rangle, \quad (9)$$

where the vector $-|i\vec{n}h\rangle$ contains the inhomogeneous terms, describing the penetrating spin waves into interface domain when appropriately decomposed onto the basis vectors.

Moreover, the scattering matrix elements give easy access to the relative reflection and transmission probabilities $r_{ii'}$ and t_{ij} of the film, at the fixed variables (Ω, ϕ_y). These are obtained by the following relations:

$$\begin{cases} r_{ii'}(\Omega, \phi_y) = (V_{gi'}/V_{gi})|R_{ii'}|^2, \\ t_{ij}(\Omega, \phi_y) = (V_{gi}/V_{gj})|T_{ij}|^2. \end{cases} \quad (10)$$

In the above equations, the group velocities of the magnons normalize the unitarity of the scattering matrix and the scattering cross sections.

To determine the total reflection and transmission cross sections in an eigenmode i, for a given doublet (Ω, ϕ_y), we add all the contributions of the scattered magnons leading to the following equation:

$$\begin{cases} r_i(\Omega, \phi_y) = \sum_{i'} r_{ii'}(\Omega, \phi_y), \\ t_i(\Omega, \phi_y) = \sum_{j} t_{ij}(\Omega, \phi_y). \end{cases} \quad (11)$$

3.2.2. *Magnonic transmittance*

To obtain the total transmission of spinwaves through the interfacial domain of the system studied, we defined the magnonic conductance or transmittance across the interface. It simply requires the addition of all the individual transmission coefficients generated by the different magnon modes, at a specific frequency Ω and a given direction (ϕ_y). Therefore, concretely we obtain,

$$\sigma(\Omega, \phi_y) = \sum_i \sum_j t_{ij}(\Omega, \phi_y). \quad (12)$$

The sum is extended to all propagating modes of magnons. The transmittance spectra $\sigma(\Omega, \phi_y)$ can be determined experimentally.

3.2.3. *Localized magnon states*

In this work, Eq. (9) connects the spin excitations and equations of motion on the boundary to the spin sites in the two perfect multilayer films joined by the interface zone.

We remind that the components of the vector $|u_{\rm int}\rangle$ are given by the amplitudes of all spin sites contained in the interface region. Furthermore, the vector connects the two subset of spin sites for the matching zones, one in the semi-infinite multilayer film on the left and the second in the semi-infinite multilayer film on the right.

A nontrivial solution of Eq. (9) means that the following determinant must be zero:

$$\det[\Omega I - D(S, r_B, r_1, r_2, r_{Bd}, r_{1d}, r_{2d}, \eta, \exp(i \times \phi_y)] = 0. \quad (13)$$

This condition permits us to establish the energies of the localized spin branches on the interface domain. They correspond to spinwaves that propagate across the shear spins joining the two semi-infinite films. The spectra are spatially localized because the precession amplitudes and the spin excitations decrease exponentially as we penetrate into the perfect multilayer films, along the x-direction.

4. Numerical Applications and Discussions

The magnon dispersion branches for the spinwaves in the multilayer perfect waveguides are presented in Fig. 2. They are plotted over the first Brillouin zone, for the alternate ferromagnetic slabs. The magnon dispersion modes are given in some direction α, as indicated in the legend. We remind that $\phi_\alpha = q_\alpha a$ defines the normalized wave vector.

In this study, the spin dispersion curves are determined and presented along the x-direction.

To identify the impact of the nature of the spin layers that make up the film, we investigated three values of the spin ration S. In addition, to examine the effect of the spin excitation direction, we considered two different incidence angles ϕ_y. The parameters used to plot the magnon dispersion curves are as follows:

— In Fig. 2(a), we considered the ration $S = 0.9$, the normal incidence $\phi_y = 0$.

— In Fig. 2(b), we take the ration $S = 1.1$, the normal incidence $\phi_y = 0$.
— In Fig. 2(c), we take the ration $S = 1.0$, the normal incidence $\phi_y = 0$.
— In Fig. 2(d), we take the ration $S = 1.0$, the oblique incidence $\phi_y = \pi/4$.

In all simulated cases, each magnon eigenmode labeled i is propagating in its specific frequency interval.

We point out that the numbering of the indices of the spin modes is performed from the bottom to the top, as indicated in the legend of Fig. 2. Moreover, while in the frequency intervals some modes are propagated, the others are evanescent modes.

In addition, there are frequency intervals where several magnon modes can be excited simultaneously. This corresponds to the zones of overlap of the modes.

For the normal incidence, defined by $\phi_y = 0$, in Figs. 2(a)–2(c), only the first two magnon modes are acoustics; they are characterized by a limiting behavior, tending to zero frequency when ϕ_x tends to zero; the eight other modes are optics, with branches that differ from zero in the Brillouin zone.

For the oblique incidence, defined by $\phi_y = \pi/4$, plotted in Fig. 2(d), there are no acoustic spin modes, but all the 10 modes are optics. In this direction, the magnon modes become more energetic.

Consequently, the orientation of the film or the incidence excitation can be used to filter the spin waves at low frequency and prevent acoustic modes.

By increasing the spin intensity S, we observe that the frequency intervals of the 10 magnon modes become wider.

To highlight the link between the group velocities (V_g) and the dispersion curves in the studied film, we have plotted, in Fig. 3, the V_g corresponding to two examples of specific parameters, indicated in Fig. 2.

In Fig. 3(a) (at the right), we have examined the case where $S = 1.0$ and $\phi_y = 0$.

In Fig. 3(b) (at the left), we simulated the situation where $S = 1.0$ and $\phi_y = \pi/4$.

It can be seen that the frequency interval where each group speed (V_{gi}, with $i = 1, \ldots, 10$) is different from zero relates well to the propagation interval of its corresponding magnon mode (i), as indicated by the dispersion curves. Furthermore, the quantity V_{gi} is equal to zero for evanescent spin modes.

Analytically, the group velocities are obtained by determining the slope of the tangent of the magnon dispersion branches plotted in the corresponding curves in Fig. 2. In order to obtain unitarity condition and the energy conservation in the waveguide, we remind that the group velocities are important to determine because they allow the normalization of the coefficients of the scattering cross sections.

From the obtained results, we can say that the magnon dispersion spectra and the group velocities depend totally on the following parameters: Exchange integral, spin intensities S_A and S_B and the incidence direction.

The main objective of this work is to study the propagation of spin waves in a multilayer film through sheared spin sites and to simulate their effects on the transmittance according to the parameters which characterize the disturbed zone.

We point out that the programs developed for our numerical calculations can be executed for all possible values of the magnetic exchange ratios defined in Eq. (1). It is important to mention that the parameters which influence the transmission and the magnonic conductance are those which characterize the interface zone itself; they are those which carry the index "d", and the others are already present for the ideal thin film without the shear.

The results of the numerical applications of the spin scattering model are presented, in Figs. 4–9, for the ordered magnetic interface zone in multilayered ferromagnetic thin film, obtained by shearing a part of the film from the other at an angle of 30°.

The spin multilayer is made of 10 slabs, achieved by alternate two spin layers A and B.

The shearing zone can be treated as an interface domain, which can significantly impact the spin excitation spectra. This is due to the fact that inhomogenous space, formed by juxtaposition of two surfaces, leads to localized interface excitations (surface magnons) and generates multiple reflections. We note that the results of the localized spin states are not presented in this paper.

In Figs. 4 and 5, we have determined, respectively, the magnon transmission, reflection spectra and its sum (Fig. 4) and the spinwave transmittance via the interface (Fig. 5), as a function of the ration of the spin intensity and magnetic exchange in the interface domain.

In the first step, we considered that the values of the spins of sites A and B are close, giving a ratio $S = 1.0$.

To simulate the impact of the magnetic coupling on the magnonic spectra, we have varied the magnetic exchange, in the boundary domain, from

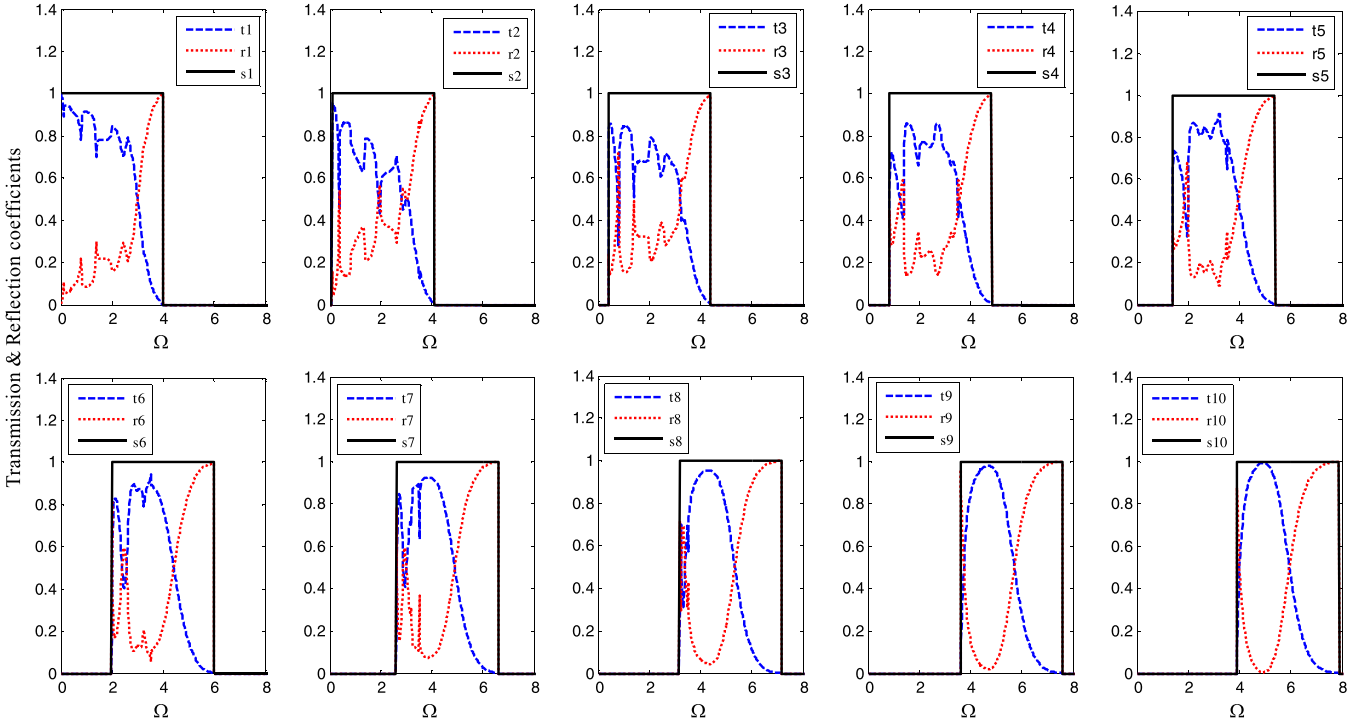

(a)

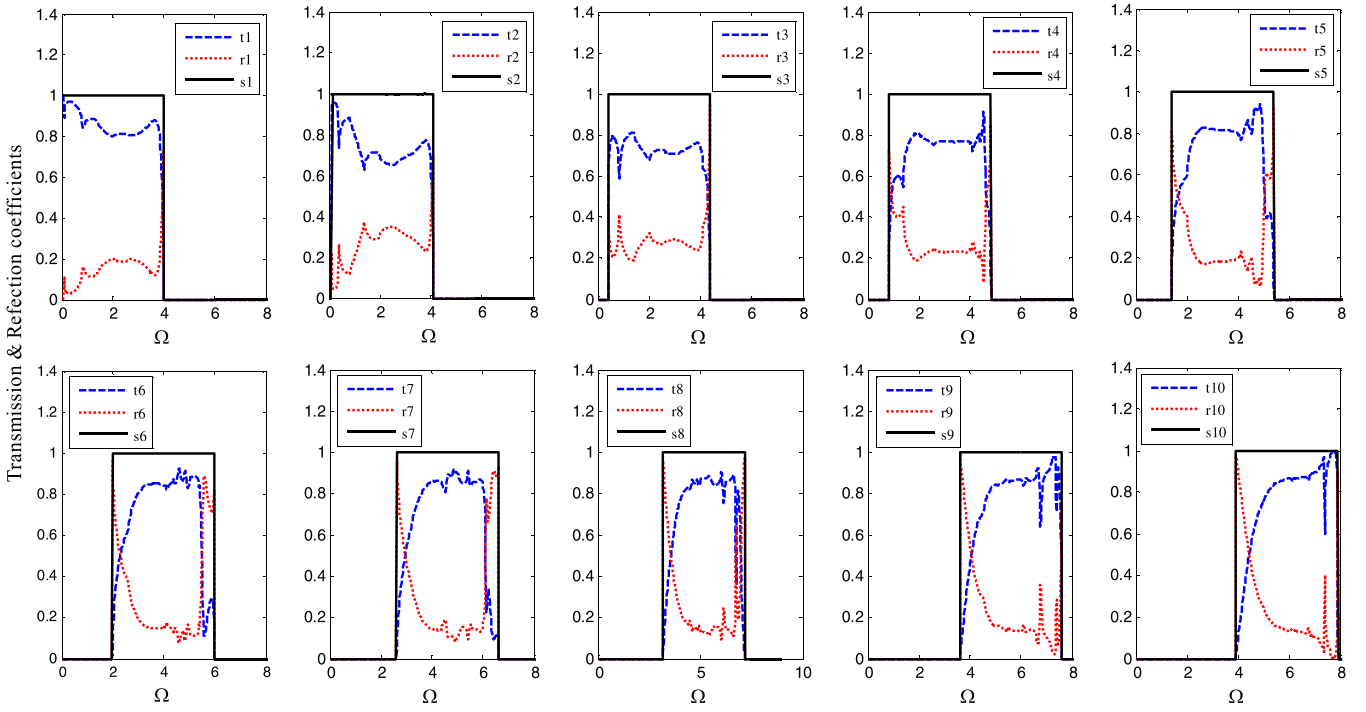

(b)

Fig. 4. The curves of transmission (dashed lines) and reflection coefficients (dotted lines) and their sum (solid lines) of the magnon modes, for the studied multilayer film. The simulations are carried out for the ratio $S = 1.0$. (The spin intensities are similar everywhere) and at the given direction $\phi_y = 0$. The spectra are plotted in the frequency interval Ω, which covers the interval propagation of all magnon modes of the perfect multilayer film. (a) The spectra describe a softening case of the spin coupling. (b) The spectra describe a hardening case of the spin coupling.

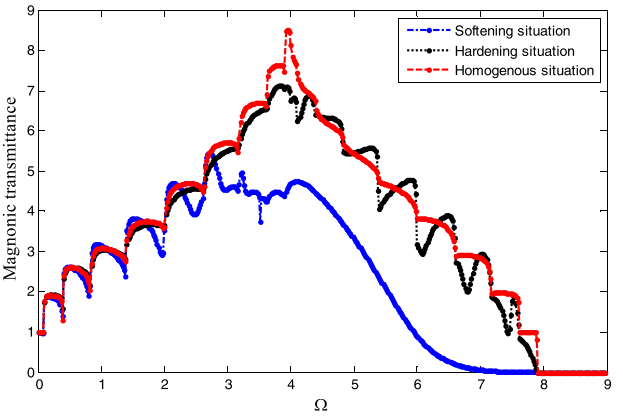

Fig. 5. Magnonic transmittance vs magnon frequency for different types of interactions: softening (dash-dotted lines), homogenous (dashed lines) and hardening case (dotted lines). The spectra are determined for the similar spin value of spin intensities $S_A = S_B$ ($S = 1.0$).

softening (Fig. 4(a)) to hardening (Fig. 4(b)). To do this, all the parameters which have the index "d" are increased (lowered) by 10% compared to those of the perfect film and this was made to study the impact of the sheared sites (the r_{Bd} ratio is also taken into consideration; it has been varied in relation to the r_B of the perfect zone with the proportions 10% greater and 10% smaller and comparable values).

In Fig. 5, the shear angle has an impact on the propagation of spin waves and it conditions the magnon transmittance. Quantized transmittance can be expected for an ideal system without any geometric deviation or defect.

Even if the values of the coupling constants are homogeneous and identical to those of the perfect system but the geometry is not similar (in particular, the number of nearest neighbors for the sheared sites is 7, unlike the perfect film which is 6); therefore, the lack of strong transmission is justified by the multiple reflections and shifting of the film configuration.

Similarly, in Figs. 6 and 7, we analyzed the configuration where the spin intensity of a spin site A is greater than the spin intensity of the site B about 10% ($S_A > S_B$).

In Figs. 8 and 9, we examined the situation when the spin intensity of a spin site A is smaller than the spin intensity of the site B about 10% ($S_A < S_B$).

For all introduced parameters, in the simulation cases, it is observed that the transmission and reflection cross sections satisfy the unitarity condition

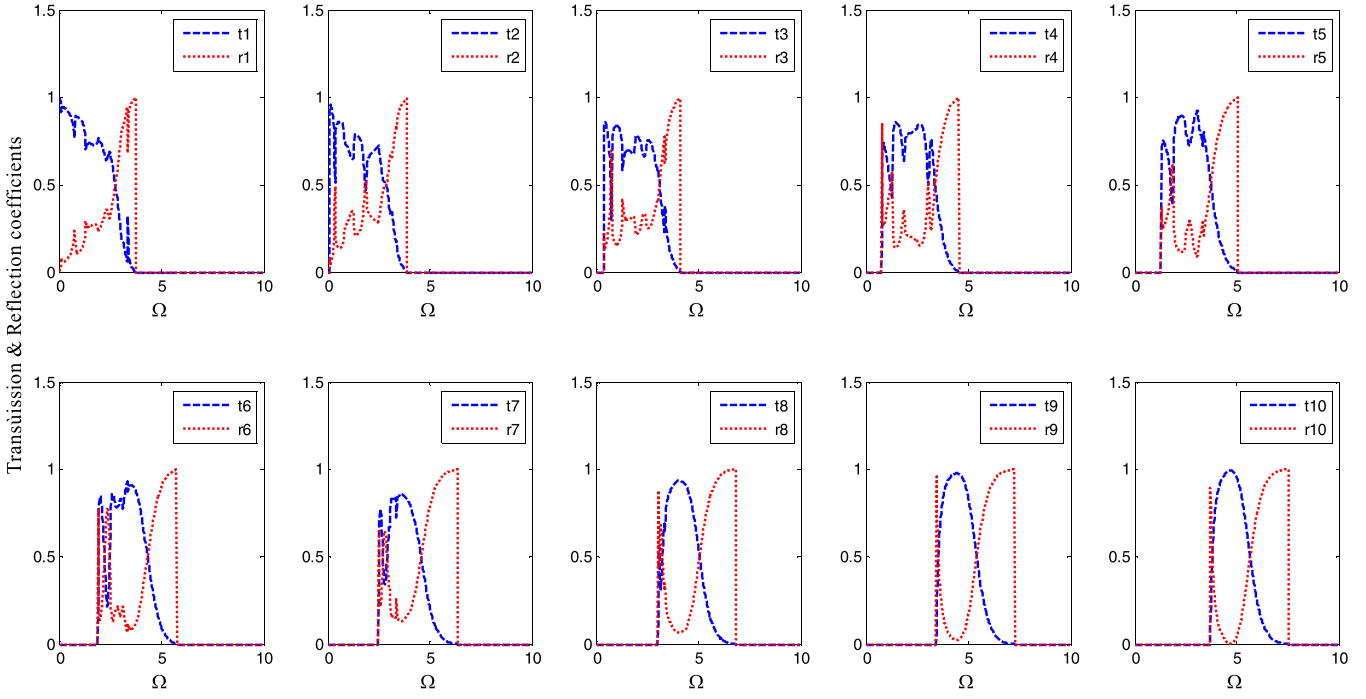

(a)

Fig. 6. As in Fig. 4, for the ratio $S = 0.9$ and the direction $\phi_y = 0$. (a) The spectra describe a softening case of the spin coupling. (b) The spectra describe a homogenous case of the spin interactions. (c) The spectra describe a hardening case of the spin coupling.

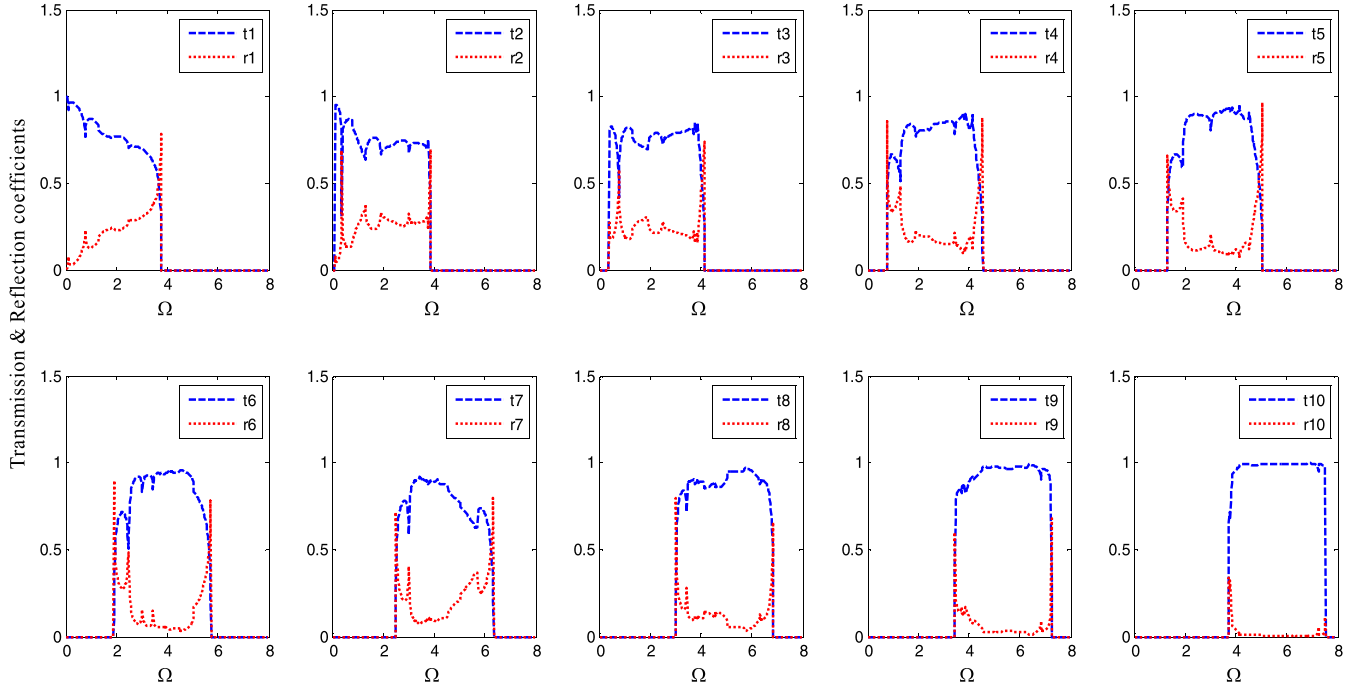

(b)

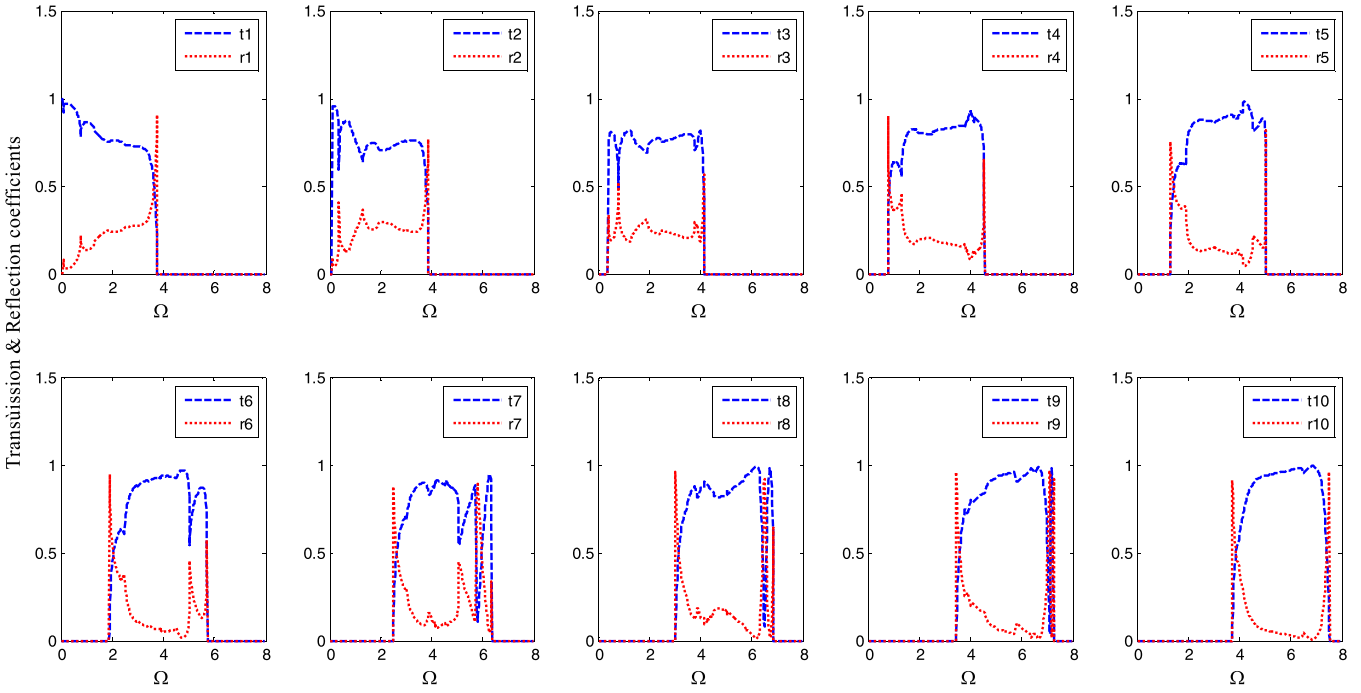

(c)

Fig. 6. (*Continued*)

of the scattering matrix ($t_i + r_i = 1$). This condition is used to control our numerical calculations.

By comparison between the magnonic spectra, plotted in Figs. 4, 6 and 8, we confirm the strong dependence of the transmission/reflection coefficients on the magnetic exchange integrals. In other words, the obtained results of magnonic spectra depend mainly on the integral of exchange, the spins S_A and S_B parameters and B and the incidence angle ϕ_y.

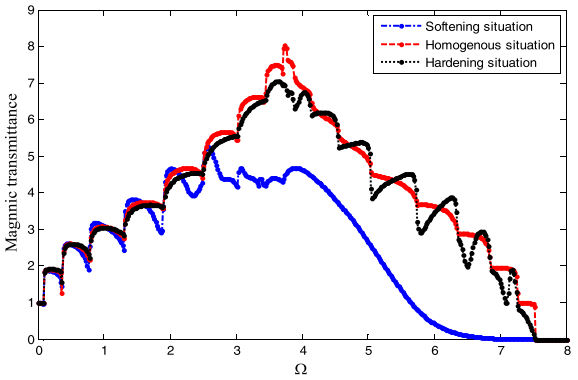

Fig. 7. As in Fig. 5, for the ratio $S = 0.9$ and the direction $\phi_y = 0$. The spin intensity of a spin site A is greater than that of the spin site B about 10% (SA > SB).

In addition, when the magnetic coupling constants, in the semi-infinite film (before the zone ensuring the scattering of the spin waves), are lower than those of the second space (located after the sheared zone), the magnons cross weakly the interface domain.

The obtained results are in conformity with our expectation, since the spinwaves cross a magnetic interface and propagate better in a slab medium with soft exchange constants. The process is reversed in the case where the magnetic interactions in the multilayer film are hard.

Due to the fact that, in any type of waves (also valid for spin waves), to cross the solid–solid interfaces more easily, it is necessary that the forces brought into play between the two subspaces located on either side of interface are weak. This situation corresponds to the softening case of the interaction constants. On the opposite case, if the medium in which the waves are diffused exhibits harsher constants than the diffusing medium, the waves are transmitted less because of energy considerations. The hardness of the coupling forces generates more reflections when crossing the zone ensuring the junction, thus leading to the decrease in transmission and conductance spectra.

It is useful to mention that, in the perfect film, the magnetic exchange constants between different spins are often expressed as a function of the concentrations of the A and B atomic sites that make up the multilayer film. Here, we consider a homogenous concentration $A_{0.5}B_{0.5}$.

It is reported that, in our simulations, we have opted for the ratios (normalization of the physical quantities) because at the interface domain, the magnetic exchanges are unavailable experimentally.

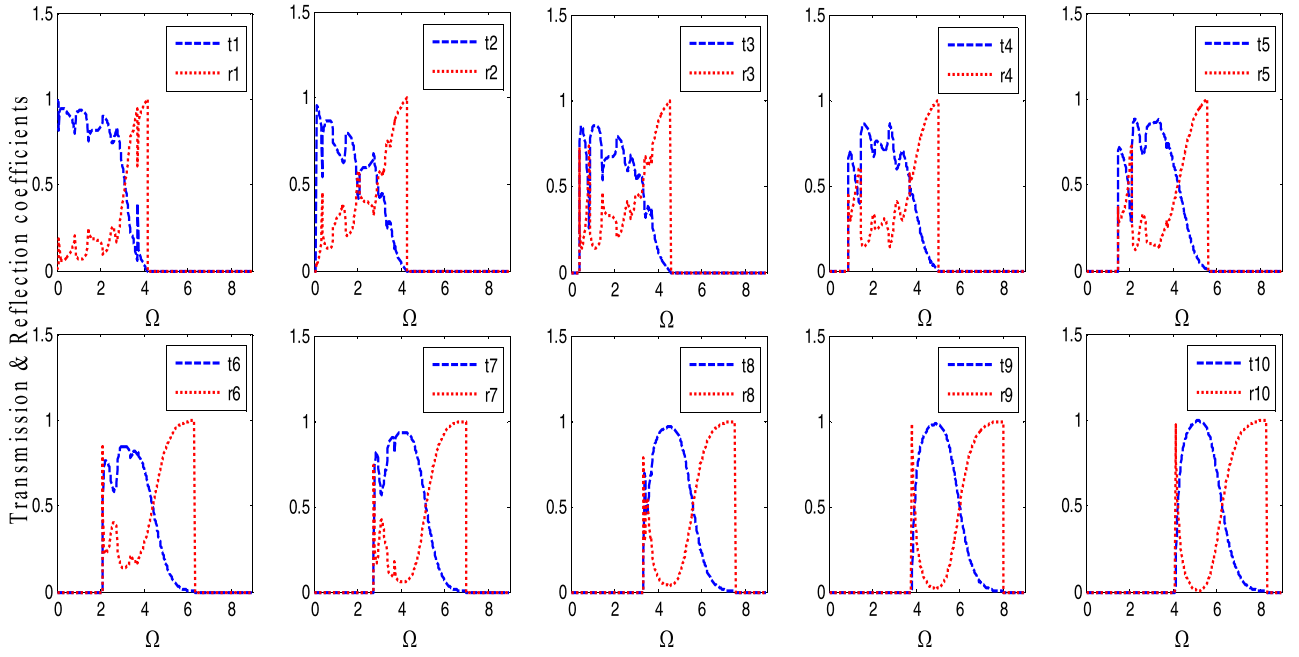

(a)

Fig. 8. As in Fig. 4, for the ratio $S = 1.1$ and the direction $\phi_y = 0$. (a) The spectra describe a softening case of the spin coupling. (b) The spectra describe a homogenous case of the spin interactions. (c) The spectra describe a hardening case of the spin coupling.

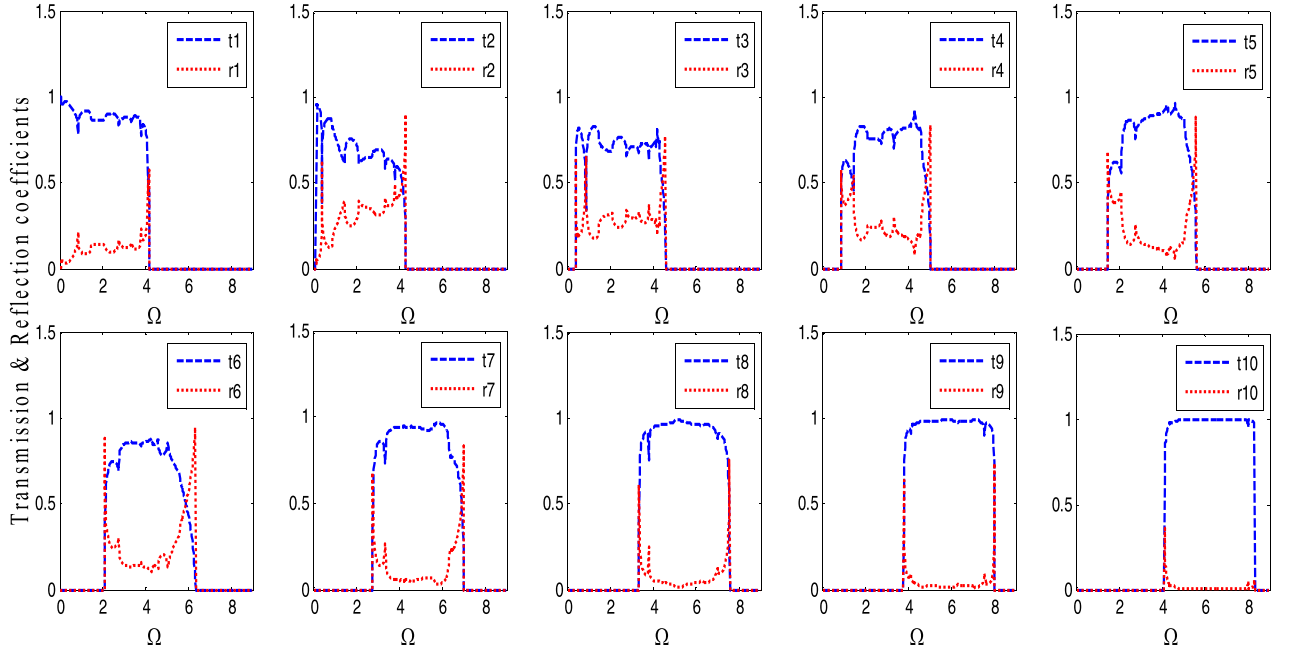

(b)

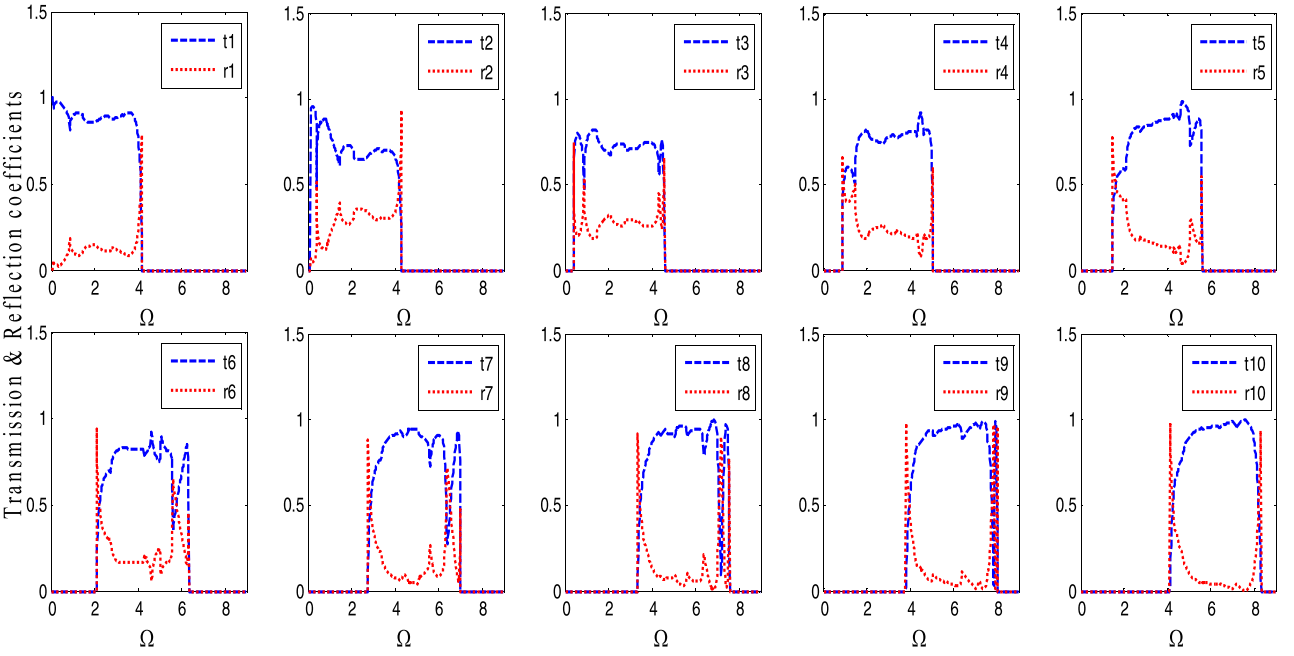

(c)

Fig. 8. (*Continued*)

Furthermore, the observed oscillations, in the three simulated possibilities of the magnetic coupling, come from the attenuation of the spin amplitude, which is generated by penetrating into the second system (in a few spin layers).

In summary, the results show that the magnonic spectra are strongly affected by the breakdown of the propagation spinwave direction. This implies the possibility of a nanometric procedure to organize the spin excitation and the magnon heat transfer from a coherent source, preferentially, into different branches of a mesoscopic system.

It is specified that we have developed computer programs which can operate with all the values entered.

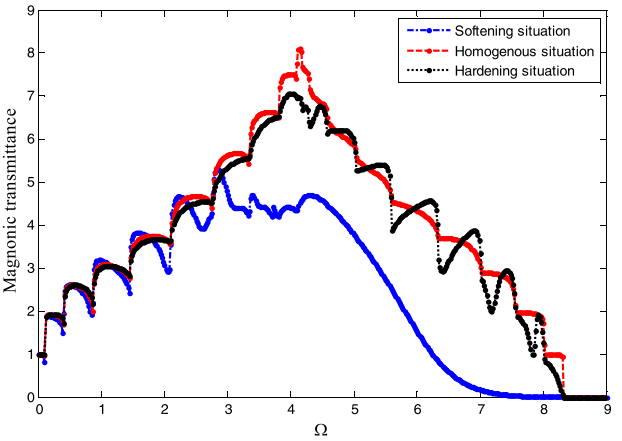

Fig. 9. As in Fig. 5, for the ratio $S = 1.1$ and the direction $\phi_y = 0$. The spin intensity of a spin site A is smaller than that of the spin site B about 10% (SA < SB).

5. Conclusion

We presented a theoretical model for the study of the magnetic properties of a ferromagnetic ordered interface in multilayer films. Accurately, we examined an interface zone obtained by shearing a part of the film from the other at an angle of 30°.

The magnon transmission and reflection spectra via the magnetic nanojunction and its spin transmittances are calculated and analyzed for different values of the intensity of spin ratio and the magnetic coupling in the interface region. The objective of changing the ratio of spin intensity is to discuss the sensitivity of the magnonic properties to the nature of the spin layer that compose the ferromagnetic film. Furthermore, our aim by varying the interatomic magnetic exchange on the interface region is to investigate the consequences of magnetic softening and hardening for the calculated properties. The results demonstrate the characteristic interference effects between incident magnons and the reflected and localized spin states on the interface zone, and the results highlight the localized spin states on the domain containing the nanojunction and their interactions with incident magnons.

The spin oscillations, observed in magnonic spectra, are attributed to the variation of the spin S and the magnetic exchange parameters at the interface domain.

Acknowledgments

The authors would like to thank S. Djebala for proofreading this paper.

This work is supported by MESRS, under the registration: PRFU-B00L02UN150120200001.

References

1. K. Ariga, Y. Yamauchi, G. Rydzek, Q. Ji, Y. Yonamine, K. C.-W. Wu and J. P. Hill, *Chem. Lett.* **43**, 36 (2014).
2. S. Srivastava and A. Kotov, *Acc. Chem. Res.* **41**, 1831 (2008).
3. A. H. Aly, H.-T. Hsu, T.-J. Yang, C.-J. Wu and C. K. Hwangbo, *J. Appl. Phys.* **105**, 083917 (2009).
4. A. L. Lacaita and A. Redaelli, *Microelectron. Eng.* **109**, 351 (2013).
5. X. Chen, Y. Zhou, V. A. L. Roy and S. T. Han, *Adv. Mater.* **30**, 1703950 (2018).
6. C. A. F. Vaz, J. A. C. Bland and G. Lauhoff, *Rep. Prog. Phys.* **71**, 056501 (2008).
7. S. Zhang, *Phys. Rev. B* **51**, 3632 (1995).
8. T. Yu, H. Yu, Y. M. Blanter and G. E. W. Bauer, *Phys. Rev. B* **99**, 134424 (2019).
9. Q. Fu, Y. Li, L. Chen, F. Ma, H. Li, Y. Xu, B. Liu, R. Liu, and Y. Du, *Chin. Phys. Lett.* **37**, 087503 (2020).
10. F. Guinea, *Phys. Rev. B***58**, 9212 (1998); L. J. Heyderman and R. L. Stamps, *J. Phys. Condens. Matter* **25**, 363201 (2013).
11. G. Belkacemi and B. Bourahla, *Int. J. Mod. Phys. B* **31**, 1750155 (2017).
12. F. Chelli, B. Bourahla and A. Khater, *Int. J. Mod. Phys. B* **34**, 2050080 (2020).
13. A. Belayadi, B. Bourahla and A. Mogari, *Spin* **9**, 1950005 (2019).
14. B. Bourahla, O. Nafa, A. Khater, *J. Supercond. Novel Magn.* **28**, 1843 (2015).
15. A. Belayadi and B. Bourahla, *Comput. Cond. Matter* **24**, e00493 (2020).
16. M. Abou Ghantous and A. Khater, *Eur. Phys. J. B* **12**, 335 (1999).
17. B. Bourahla, A. Khater, R. Tigrine, O. Rafil and M. Abou Ghantous, *J. Phys. Cond. Matter* **19**, 266208 (2007).
18. A. Khater, L. Saim, R. Tigrine and D. Ghader, *Surf. Sci.* **672–673**, 47 (2018).
19. L. Barbier, A. Khater, B. Salanon and J. Lapujoulade, *Phys. Rev. B* **43**, 14730 (1991).
20. L. J. Jiang and M. G. Cottam, *J. Appl. Phys.* **85**, 5495 (1999).
21. T. E. Feuchtwang, *Phys. Rev.* **155**, 731 (1967).
22. J. Szeftel and A. Khater, *J. Phys. C. Solid State Phys.* **20**, 4725 (1987).
23. J. Szeftel, A. Khater, F. Mila, S. d'Addato and N. Auby, *J. Phys. C. Solid State Phys.* **21**, 2113 (1988).
24. M. Tamine, *J. Magn. Magn. Mat.* **153**, 366 (1996).

25. M. Belhadi and R. Chadli, *Surf. Rev. Lett.* **11**, 321 (2004).
26. A. Khater, B. Bourahla, M. Abou Ghantous, R. Tigrine and R. Chadli, *Eur. Phys. J. B* **82**, 53 (2011).
27. M. Belhadi and A. Khater, *Surf. Rev. Lett.* **16**, 55 (2009).
28. B. Bourahla and O. Nafa, *Spin* **6**, 1650007 (2016).
29. D. Ghader and A. Khater, *J. Magn. Magn Mat.* **482**, 88 (2019).